INTERNATIONAL JOURNAL OF HYDROGEN ENERGY

Enhanced hydrogen uptake/release in 2LiH–MgB_2 composite with titanium additives

Ivan Saldan [a,b]*, Renato Campesi [c], Olena Zavorotynska [d], Giuseppe Spoto [d], Marcello Baricco [d], Anna Arendarska [a], Klaus Taube [a], Martin Dornheim [a]

[a] *Institute of Materials Research, Helmholtz Zentrum Geesthacht, 1 Max-Planck Str., D-21502 Geesthacht, Germany*

[b] *Institute for Energy Technology, Physics Department, Instituttveien 18, Kjeller 2027, Norway*

[c] *Institute for Energy, Joint Research Centre, NL-1755 ZG Petten, The Netherlands*

[d] *NIS Centre of Excellence, Department of Chemistry, University of Torino, Via P. Giuria 7, I-10125 Torino, Italy*

ABSTRACT

The influence of different titanium additives on hydrogen sorption in LiH–MgB_2 system has been investigated. For all the composites LiH–MgB_2–X (X = TiF_4, TiO_2, TiN, and TiC), prepared by ball milling in molar ratios 2:1:0.1, five hydrogen uptake/release cycles were performed. In-situ synchrotron radiation powder X-ray diffraction (SR-PXD) and attenuated total reflection infrared spectroscopy (ATR-IR) have been used to characterize crystal phases developed during the hydrogen absorption-desorption cycles.

All the composites with the titanium additives displayed an improvement of reaction kinetics, especially during hydrogen desorption. The LiH–MgB_2–TiO_2 system reached a storage of about 7.6 wt % H_2 in ~ 1.8 hours for absorption and ~ 2.7 hours for desorption. Using in-situ SR-PXD measurements, magnesium was detected as an intermediate phase during hydrogen desorption for all composites. In the composite with TiF_4 addition the formation of new phases (TiB_2 and LiF) were observed. Characteristic diffraction peaks of TiO_2, TiN and TiC additives were always present during hydrogen absorption-desorption. For all as-milled composites, ATR-IR spectra did not show any signals for borohydrides, while for all hydrogenated composites B–H stretching (2450–2150 cm^{-1}) and B–H bending (1350–1000 cm^{-1}) bands were exactly the same as for commercial $LiBH_4$.

Keywords: hydrogen uptake/release reaction, 2LiH–MgB_2 composite, titanium additive.

I.Saldan*
Institute for Energy Technology
Physics Department
IFE, Instituttveien 18, Kjeller 2027, Norway
Tel:+47 6380-6079
Fax:+47 6381-0920
E-mail: ivan_saldan@yahoo.com

1. Introduction

Hydrogen can be one of the alternative energy carriers, which should replace the traditional fossil fuels in a nearly future. One of the promising materials for hydrogen mobile application which has been studied approximately for 10 years is $LiBH_4$ [1]. Having high gravimetric and volumetric hydrogen density, this material, though, exhibits unfavorable kinetics and thermodynamics for real application in fuel cells. Recently, it was found that $LiBH_4$ can be destabilized by the addition of MgH_2, showing better decomposition kinetics with respect to the pure compound [2]. A detailed analysis of the reversible interaction between $LiBH_4$ and MgH_2 was made in [3] and can be summarized as follow:

$$2\ LiBH_4 + MgH_2 \leftrightarrow 2\ LiBH_4 + Mg + H_2 \leftrightarrow 2\ LiH + MgB_2 + 4H_2 \quad (1)$$

The direct reactions (1) take place at ~ 400 ºC. Opposite reactions, with simultaneous formation of $LiBH_4$ and MgH_2 under 50 bar of H_2, was confirmed at the temperatures 250–300 ºC [3]. It was observed that suitable additives might decrease reaction temperatures and improve kinetics of (1). Experimental evidence of kinetic improvement for reversible middle-temperature Na, Li and Al based complex hydrides doped by titanium additives appeared in 1997 [4]. It has also been reported that the kinetic improvement of the reaction (1) was reached by addition of 1 mol% of TiF_3 [5]. The property enhancement arising upon this additive persists well in the subsequent hydrogen uptake/release cycles. Another prominent example of the additives effect was the composite $LiBH_4$–MgH_2–$Ti\{OCH(CH_3)_2\}_4$ mixed in molar ratio 2:1:0.1 [6]. After ball milling TiO_2 anatase was found and during 1-st hydrogen desorption Ti_2O_3 and TiB_2 appeared to be stable after cycling. XPS analysis showed that the reduction of Ti (IV) to Ti(III) was coupled with the migration of titanium species from the surface into the bulk of the composite. The role of additives and microstructure refinement in $LiBH_4$–MgH_2 system were studied in [7,8], revealing that two main factors, proposed as potential driving force for kinetic improvement, were related to (i) favoring heterogeneous nucleation of MgB_2 and (ii) increasing of interfacial area trough grain refinement. Titanium diboride (TiB_2) has the same hexagonal lattice structure as MgB_2 with very small (1.85 %) directional and interplanar misfit. This fact is a necessary condition for heterogeneous nucleation of MgB_2 because of the interfacial energy lowering. The appropriate concentration of the additive and its homogeneous distribution were found to be the main conditions for the efficient heterogeneous nucleation of MgB_2. However because of no change of the limiting rate neither for hydrogen absorption (contracting volume model) nor for desorption (interfaced-controlled one-dimensional growth) [8], induced by the additives, the latter do not show catalytic behavior. The theoretical work [9] has shown that thermodynamic stability of point defects in complex hydrides defines the ground or intermediate states or the driving force for atomic motion. Incorporation of Ti cations in $LiBH_4$ is energetically unfavorable suggesting that only surface effect takes place.

In order to understand thoroughly the effect of titanium additives, where metallic part is Ti and non-metal is the element of 2-nd period of the Periodic Table from F to C, we have started a systematic investigation. In this work the study on the influence of several titanium additives (TiF_4, TiO_2, TiN and TiC) on reversible hydrogen reactions in 2LiH–MgB_2 system during five hydrogen uptake/release cycles is presented.

2. Experimental details

Commercial LiH (≥95%, Sigma Aldrich) and MgB_2 (>96%, Alfa Aesar) powders were used to prepare composite with titanium additives in molar ratios 2:1:0.1, respectively. TiF_4 (98%, Alfa Aesar), TiO_2 (rutile, 99.7%, Sigma Aldrich), TiN (97.7%, Alfa Aesar) and TiC (99.5%, Alfa Aesar) were chosen as additives. The composites of powders were high-energy milled for 5 h using Spex 8000 M Mixer Mill in argon atmosphere. Stainless steel balls 10 mm in size with 10:1 ratio balls to powders were used.

Hydrogen sorption measurements were carried out in a commercial Sievert's type apparatus (PCTpro 2000). The milled composites were hydrogenated under 50 bar of hydrogen pressure at 330 or 350 ºC in a special high pressure-temperature sample holder. Hydrogen desorption was performed under 5 bar back pressure of hydrogen at 380 ºC, after previous absorption. Five complete hydrogen uptake/release cycles were performed.

In situ SR-PXD was performed in D3 beamline at DESY Hamburg (Germany). The samples were airtight encapsulated in sapphire capillaries to be installed in a special in situ SR-PXD cell; further details are described in [10]. Samples after complete 1-st hydrogen absorption were heated at 5 °C/min from room temperature up to 380 °C and kept in isothermal conditions for 2 hours and then cooled down to room temperature. All handling and preparation of materials took place in a glove-box with continuously purified argon atmosphere and oxygen and moisture values were less than 1 ppm.

ATR-IR (Attenuated total reflection infrared) spectra were taken with a Brüker-ALPHA Platinum spectrometer with ATR diamond crystal accessory. The spectra were recorded in 4000-375 cm^{-1} range with 2 cm^{-1} resolution. Sixty four scans were averaged for background and sample spectra. All the measurements were carried out in the nitrogen filled glove-box with oxygen and moisture levels less that 0.1 ppm.

3. Results and discussion

3.1. Hydrogen uptake/release cycling

As a reference, a complete hydrogen uptake/release cycle for the LiH–MgB_2 system without any additive has been performed. In Fig. 1, the results of volumetric analysis of hydrogen absorption at 350 ºC and 50 bar H_2 and desorption at 380 ºC and 5 bar H_2 for LiH–MgB_2 in molar ratio 2:1 are presented.

Fig. 1 Hydrogen sorption for LiH–MgB_2 in molar ratio 2:1. Conditions for absorption and desorption were 350 ºC at 50 bar H_2 and 380 ºC at 5 bar H_2, respectively.

The reaction rate of hydrogen absorption and desorption is approximately six times different: ~ 20 hours are required for hydrogenation (~ 8.7 wt % H_2) and more than 120 hours for complete dehydrogenation. A two-step hydrogen release was observed, displaying: approximately ~ 2.3 wt % H_2 from MgH_2 and ~ 6.4 wt % H_2 from $LiBH_4$ decomposition. Absorption curve is very similar to that obtained in [11] at the same conditions. Probably, due to a slightly smaller desorption temperature (400 ºC in [11] and 380 ºC in present work) the process in our case was much slower although it showed the same two-step reaction.

The 1-st hydrogen absorption-desorption cycle in the LiH–MgB_2–TiF_4 system (Fig. 2) showed similar hydrogen absorption time (~ 20 hours) but lower gravimetric capacity (~ 7.5 wt % H_2) compared to that of the

unmodified LiH–MgB_2 (Fig. 1). Because of slower reactions at the 1-st cycle (1-st hydrogen absorption and 1-st desorption), an activation process could take place. It might be explained by grain refinement in solid material under repeating of hydrogen sorption reactions. After that, the system displays three-step reversible reaction (~ 2.3 wt % H_2 in ~ 0.7 h; ~ 6.6 wt % H_2 in ~ 2.2 h; and further to be complete) and (~ 2.3 wt % H_2 in ~ 0.6 h; ~ 7.4 wt % H_2 in ~ 5.4 h; and further to be complete) on hydrogen absorption and desorption, respectively. It can be concluded that the rate of hydrogen absorption and desorption at various steps is increased because of the addition of TiF_4 to the LiH–MgB_2 system, though hydrogen storage capacity was lowered by 1.2 wt % H_2.

Fig. 2 Hydrogen sorption for LiH–MgB_2–TiF_4 in molar ratio 2:1:0.1 during 5 cycles. Absorption (*a*) at 350 ºC and 50 bar H_2; desorption (*b*) at 380 ºC and 5 bar H_2.

For the LiH–MgB_2–TiO_2 system, at least two cycles were necessary to stabilize hydrogen absorption-desorption properties (Fig. 3). After the 2-nd cycle, the system showed ~ 8.1 wt % H_2 hydrogen storage capacity after ~ 10 h of hydrogenation. Beginning from 3-rd cycle two reaction steps were very well distinguished and resulted to ~ 7.6 wt % H_2 in ~ 1.8 h and 2.7 h for hydrogen absorption and desorption, respectively. In this case, rates for hydrogen absorption and desorption are rather similar. During the 1-st cycle, LiH–MgB_2–TiO_2 showed the same value of hydrogen gravimetric density as the unmodified LiH–MgB_2 but with faster kinetics.

Fig. 3 Hydrogen sorption for LiH–MgB_2–TiO_2 in molar ratio 2:1:0.1 during 5 cycles. Absorption (*a*) at 330 ºC and 50 bar H_2; desorption (*b*) at 380 ºC and 5 bar H_2.

The results of hydrogenation/dehydrogenation reactions in the LiH–MgB_2–TiN system are shown in Fig. 4. After the 1-st cycle, the process is stable and requires ~ 20 hours to reach the maximum gravimetric capacity of ~ 8.0 wt % H_2. The hydrogenation curve does not show distinctive steps, however during the hydrogen desorption three separate steps are clearly visible. The 4-th desorption cycle displays only two steps (~ 2.6 wt % H_2 in ~ 0.5 h; ~ 7.9 wt % H_2 in ~ 9.2 h); and the process is not completed. The LiH–MgB_2–TiN system, indeed, showed 12 times faster desorption rate than the unmodified LiH–MgB_2, though hydrogen storage capacity was reduced by ~ 0.7 wt % H_2.

Fig. 4 Hydrogen sorption for LiH–MgB_2–TiN in molar ratio 2:1:0.1 during 5 cycles. Absorption (*a*) at 330 ºC and 50 bar H_2; desorption (*b*) at 380 ºC and 5 bar H_2.

For the LiH–MgB_2–TiC system at least four cycles were needed in order to have a stable hydrogen uptake/release reaction. Hydrogen storage capacity of ~ 7.0 wt % H_2 within ~ 20 h was achieved at the 5-th cycle (Fig. 5). Only for hydrogen desorption it was possible to distinguish the first step (~ 2.0 wt % H_2 in ~ 0.5 h; and further to be complete). We conclude that, among all presented system with titanium additives, the LiH–MgB_2–TiC one showed the major reduction in hydrogen storage capacity (~ 1.7 wt % H_2), though much higher hydrogen desorption rates were observed with respect to the unmodified LiH–MgB_2 system.

Fig. 5 Hydrogen sorption for LiH–MgB_2–TiC in molar ratio 2:1:0.1 during 5 cycles. Absorption (*a*) at 330 ºC and 50 bar H_2; desorption (*b*) at 380 ºC and 5 bar H_2.

In conclusion, all titanium additives in the LiH–MgB_2–X systems (X = TiF_4, TiO_2, TiN and TiC) demonstrated kinetic improvement, especially during hydrogen desorption. The system with the TiO_2 additive showed faster rates for both hydrogen uptake and release, together with the lowest decrease in hydrogen storage capacity (~ 0.6 wt % H_2). One important note that should be mentioned in this subtitle is the value of hydrogen absorption and desorption capacity. Theoretically, during hydrogen uptake/release cycling the value of hydrogen storage capacity must be exactly the same as under complete absorption or desorption, of course if the system is stable. In present results (Fig. 1-5) quite often a small uncertainties were present where hydrogen capacity under desorption was higher than that under absorption. It might be explained by a shorter incubation period before the system start to react, especially in the next cycles. It is suggested that during manual switching from dehydrogenation to hydrogenation some amount of hydrogen could be absorbed when data acquisition had not been active yet.

3.2. In-situ SR-PXD for LiH–MgB_2–X (X = TiF_4, TiO_2, TiN, TiC) systems

For all hydrogenated LiH–MgB_2–X (X = TiF_4, TiO_2, TiN, TiC) systems in-situ SR–PXD analysis was performed (Fig. 6). Traces of MgB_2 were found in all the samples after 1-st hydrogen absorption, suggesting that the hydrogenation process was not completed. At the beginning of first hydrogen desorption reaction, pure magnesium phase was clearly visible, confirming the occurrence of a two-step reaction (1).

Fig. 6 In-situ SR-PXD under 5 bar H_2 of LiH–MgB_2–TiX (X = TiF_4 (*a*); TiO_2 (*b*); TiN (*c*); TiC (*d*)) in molar ratio 2:1:0.1 composites after complete 1-st hydrogen absorption.

In the LiH–MgB_2–TiF_4 system (Fig. 6*a*), after the 1-st hydrogen absorption step, the expected products ($LiBH_4$ and MgH_2) were present as the main phases. In addition, new phases TiB_2 and LiF were detected in the sample, whereas there was no evidence of present TiF_4. Most probably, LiF formed during milling (similar to TiF_3 in [5]) by the following reaction:

$$4\ LiH + TiF_4 \rightarrow 4\ LiF + TiH_2 + H_2 \quad (2)$$

And TiH_2 can easily react at higher temperatures with $LiBH_4$ to produce TiB_2 (estimated reaction enthalpy is ~6.5 kJ/mol H_2):

$$2\ LiBH_4 + TiH_2 \rightarrow 2\ LiH + TiB_2 + 4\ H_2 \quad (3)$$

Upon heating the hydrogenated LiH–MgB_2–TiF_4 composite started hydrogen desorption through MgH_2 decomposition and Mg formation just before isothermal conditions. During the heat treatment two diffraction peaks characteristic of a cubic phase appeared. These peaks were quite broad, likely due to the superposition of reflections due to LiH and LiF phases. Upon cooling, the peaks of o-$LiBH_4$ reappeared. It should be denoted that, after the isothermal treatment of 2 hours at 380 ºC, no diffraction peaks due to MgH_2 or Mg phases were detected, suggesting that after this period the first step of the reaction (1) was completed.

The SR-PXD pattern of the LiH–MgB_2–TiO_2 system (Fig. 6*b*) after 1-st hydrogen absorption showed diffraction peaks due to the products of the reversible reaction (1) ($LiBH_4$ and MgH_2), together with a small amount of residual MgB_2. Most of TiO_2 peaks were present during whole SR-PXD experiment. It means that this additive might be chemically inert toward the reagents. During heating of the hydrogenated mixture, hydrogen desorption started just before 380 ºC, as it was already observed for the previous composite, showing pure magnesium as intermediate. After cooling, no diffraction peaks related to Mg or MgH_2 phases were observed.

The pattern of the LiH–MgB_2–TiN system (Fig. 6*c*) showed diffraction peaks due to the products of reactions (1), similarly to the previous cases, together with evidence of the parent TiN phase. The additive was present during the whole SR-PXD measurement, confirming that no chemical reactions between the additive and the hydrides took place. Overall, the behavior of LiH–MgB_2–TiN sample under heating and cooling was similar to that observed for LiH–MgB_2–TiO_2 mixture.

The LiH–MgB_2–TiC system (Fig. 6*d*) also showed the products of hydrogen absorption-desorption and unreacted titanium-based additive, similarly to the case of LiH–MgB_2–TiO_2 and LiH–MgB_2–TiN mixtures. Four diffraction peaks of TiC phase, indeed was observed SR-PXD patterns, confirming that the additive does not react with the hydrides.

Based on SR-PXD observations, it can be concluded that only TiF_4 additive was chemically reacting in the composite during ball milling, so that the new LiF and TiB_2 phases were formed.

3.3. ATR-IR spectroscopy of milled and hydrogenated LiH–MgB_2–X (X = TiF_4, TiO_2, TiN, TiC) systems

Infrared spectroscopy is a suitable tool for characterisation of metal borohydrides since the molecular vibrations of $[BH_4]^-$ group are readily distinguishable in the spectrum. Furthermore, the normal modes of $[BH_4]^-$ group are very sensitive to the surrounding so that the alterations in a borohydride chemical composition, lattice symmetry, and the bond type can be identified in the spectrum (see reference [12] and references therein). Free $[BH_4]^-$ species belong to T_d symmetry point group with four normal modes of vibration: $\bar{\nu}_1$, $\bar{\nu}_2$, $\bar{\nu}_3$, and $\bar{\nu}_4$, out of which the latter two triply degenerate modes are IR-active. The B-H stretching modes ($\bar{\nu}_1$, $\bar{\nu}_3$) of $[BH_4]^-$ fall in the 2500-2100 cm^{-1} region, H-B-H bending vibrations ($\bar{\nu}_2$, $\bar{\nu}_4$) can be observed in the 1200-900 cm^{-1} region. In the *Pnma* space group of $LiBH_4$, the site symmetry of $[BH_4]^-$ species is lowered till C_s, all modes become IR-active, and the degeneracy of normal modes is removed, giving rise to additional peaks in the spectra [13]. In this way, the IR spectrum of $LiBH_4$ is indeed a unique fingerprint of this solid.

The ball-milled LiH–MgB_2–X (X = TiF_4, TiO_2, TiN, TiC) composites were tested by ATR before and after hydrogenation, in order to verify the formation of $LiBH_4$. ATR spectra for the as-prepared composites are shown in Fig. 7. The spectrum of LiH is also reported for comparison. The spectrum of LiH is characterised by a large absorption in the <1200 cm^{-1} region, due to the vibrations of the crystal lattice. It can be readily seen that this absorption is also present in all the LiH–MgB_2–X composites. It is also straightforward that $LiBH_4$ is not formed during ball-milling process, since no characteristic vibrations in 2500–2100 cm^{-1} and the 1200–900 cm^{-1} regions are present. All the composites have the baseline absorption steadily increasing at the lower frequencies, which is characteristic for MgB_2 (Fig. S1). No absorption peaks of TiF_4 at ca. 750 cm^{-1} (see Fig. S1 in Supporting information) are observed in the composite with TiF_4 additive. The weak peaks at ca. 2800–3000 cm^{-1} and at ca. 1600–1400 cm^{-1} correspond to molecular vibrations of organic compounds (e.g. C–H stretching and

bending of $–CH_3$ groups in aliphatic hydrocarbons; C=O groups, –C–O–C– groups, etc.). These carbon species were likely originated during ball-milling, where vials were cleaned with ethanol and a rubber O-ring was used as a gasket for sealing.

Fig. 7 ATR-IR spectra of LiH–MgB_2–X (X = TiF_4, TiO_2, TiN, TiC) systems after ball-milling. The reference spectrum of LiH is also shown. Spectra are translated along the Y axis for better representation.

The IR-ATR spectra of ball-milled LiH–MgB_2–X (X = TiF_4, TiO_2, TiN, TiC) composites after 1-st hydrogen absorption are presented in Fig. 8.

Fig. 8 ATR-IR spectra of LiH–MgB_2–X (X = TiF_4, TiO_2, TiN, TiC) systems after 1-st hydrogen absorption. The reference spectrum of $LiBH_4$ is also shown. Spectra are translated along the Y axis for better representation.

The characteristic $[BH_4]^-$ vibrational profile of $LiBH_4$ is readily observable in the spectra of all hydrogenated composites. In general, the spectra of $LiBH_4$ formed in the hydrogenation composites are similar to that one of the commercially available reference, where the different components of $\bar{\nu}_2$, $\bar{\nu}_3$, and $\bar{\nu}_4$ normal modes are clearly distinguishable. The $\bar{\nu}$ mode is very weak in the IR spectrum and falls in the region of the strong $\bar{\nu}_3$ mode, such as it cannot be observed in the spectrum. In the spectrum of the composite doped with TiC, an additional peak at 1120 cm^{-1}, marked with the asterisk on Fig. 9, appears. This peak, however, rather belongs to the impurities that to the modifications in $LiBH_4$, since all other principle modes remain almost unaffected. As the vibrational profile of $[BH_4]^-$ is almost the same in the spectra of all the composites, we can conclude that pure $LiBH_4$ is formed in these samples after hydrogenation. The strong absorption due to LiH in the < 1200 cm^{-1} region, as on the Fig. 7, is not present, which evidences the disappearance of LiH phase from these samples after hydrogenation.

The increase in baseline absorption (comparing to that of the pure $LiBH_4$) in the spectra of the hydrogenated composites evidences the presence of some binary compounds. As it can be clearly seen on Fig. 9, the baselines of all the hydrogenation composites fit well with the vibrational profile of MgH_2.

Fig. 9 Low energy region ATR-IR spectra of LiH–MgB_2–X (X = TiF_4, TiO_2, TiN, TiC) systems after the 1-st hydrogen absorption: spectra 1-3 correspond to the composites with TiO_2, TiC, and TiF_4, respectively, spectrum 4 corresponds to the composite with TiN additive.

Among the four composites, those with TiF_4, TiO_2, and TiC (spectra 1-3 in Fig. 9) have very similar baseline profiles in the low energy region of the ATR-IR spectra, whereas the composite with the TiN additive (spectrum 4) obviously has some additional absorption, which has the best fit with the vibrational profile of TiN (the ATR spectra of other reference compounds can be found in the Fig. S1 of the Supporting information). Even after hydrogenation, no absorption peaks due to TiF_4 at ca. 750 cm^{-1} are observed in the composite with TiF_4 additive. It is not possible to identify the presence of other phases, (LiF, TiB_2, TiO_2, TiC, Ti) from these spectra, since they all have rather similar profile in the low region (Fig. S1), however, their presence cannot be excluded. Our conclusions are supported by the SR-PXD results.

Fig. S1 ATR-IR spectra of reference compounds.

3.4 General discussion

Theoretically a general catalytic mechanism for reaction between $LiBH_4$ and MX_n additive (where M is metal with n valence; X is halogen) would be presented as follows:

$$n\ LiBH_4 + MX_n \rightarrow n\ LiX + M(BH_4)_n \quad (4)$$

$$n\ LiX + M(BH_4)_n \rightarrow n\ LiX + MB_n + 2n\ H_2 \quad (5)$$

$$n\ LiX + MB_n + 2n\ H_2 \rightarrow MX_n + n\ LiH + n\ B + 2n\ H_2 \quad (6)$$

This mechanism was observed in case of solid state reaction between $LiBH_4$ and $TiCl_3$. [14, 15] The reaction occurs at room temperature with the formation of LiCl. Similar result was observed in [16] for the interaction between $LiBH_4$ and $TiCl_4$:

$$4\ LiBH_4 + TiCl_4 \rightarrow Ti(BH_4)_3 + 4\ LiCl + 1/2\ B_2H_6 + 1/2\ H_2 \quad (7)$$

It was concluded that the dehydrogenation temperatures of $Ti(BH_4)_3$ was ~ 298 K. Thus, at room temperature and ambient pressure $Ti(BH_4)_3$ decomposes releasing hydrogen and possibly trace amounts of gaseous B_2H_6. Similar ion-exchange interactions (4) could take place in case of $LiBH_4$ with $MgCl_2$ [17], $MnCl_2$ [18] or ZnF_2 [19], and as in the present paper, with TiF_4. In case of RHCs, based on lithium borohydride, the additives likely react with $LiBH_4$ in similar way. However, MgH_2 plays an additional role in the kinetic improvement [9]. In our experiment, because of the higher temperature of $LiBH_4$ crystallization, $Ti(BH_4)_3$ was not found as a product of reaction (4) but the formation of LiF was confirmed.

As established by SR-PXD experiments, TiO_2, TiN and TiC did not react with the composites. Therefore they could only catalyze hydrogen sorption kinetics. It should be mentioned that transition metal oxides are more promising additives for hydrogen kinetics than pure transition metals though the latter have orders of magnitude higher activity to molecular hydrogen dissociation [21-25]. Obviously, the explanation of catalytic effect by metal oxides should be found by tools of surface science. Indeed, the interaction of high surface area oxides (alumina, titania or their mixtures) with gas has been widely studied in heterogeneous catalysis. With respect to alumina or titania, the single phase alumina-titania solid acids [26] have stronger acid sites and higher acid site density. These facts, coupled with their high surface area produce the materials with an even larger number of acid sites per gram, making them useful in heterogeneous catalysts. Probably, for TiN and TiC catalytic effects also can be explained by their surface activity towards the molecular hydrogen since no chemical reactions with these additives were found.

Because of high reactivity of $LiBH_4$, it is not easy to find an additive which is not consumed by chemical reaction. In most cases, proposed in literature additives behave as reagents producing intermediates but finally cannot be recovered to the parent reactants. For TiF_4, TiO_2, TiN and TiC, depending on the non-metal, the standard enthalpy of formation are –1649.3; –944.0; –338.1 and –184.5 kJ/mol, respectively [27]. Depending on the free energy for the possible interactions between the additives and LiH or $LiBH_4$, their behavior can be different: chemical, physical etc. However, the kinetics of hydrogen sorption is related to the surface properties of the additives. We suppose that chemically unreacted titanium additives (TiO_2, TiN and TiC) could be the

"active surface centers", where dissociation of molecular hydrogen under hydrogenation and association of atomic hydrogen under dehydrogenation can be accelerated.

In recent work [28] the investigation of the effect of Ti, TiH_2, TiB_2, $TiCl_3$, and TiF_3 additives on the hydrogen sorption kinetics in LiH/MgB_2 mixture has been done. There it was concluded that all these titanium additives effectively decrease the onset temperature of hydrogenation. Similar to our present results, the TiH_2, TiB_2, $TiCl_3$, and TiF_3 additives were mostly responsible for faster hydrogen desorption kinetics and only metallic titanium in $LiH–MgB_2$ composite actively participates in both hydrogenation and dehydrogenation process [28]. This is again the confirmation of more pronounced role of anion (the more electronegative atom in titanium additives) at association of atomic hydrogen than dissociation of molecular hydrogen. From another hand, based on the measurements for $LiBH_4–MgH_2$ composite catalysed by $TiCl_3$, $ZrCl_4$ and $HfCl_4$ additives in [29], we suggest that regards to hydrogen desorption Ti cation might be the most significant element among all of IVB group in Periodic Table. In conclusion of the discussion, it would be reasonable to proceed the studying about the effects of titanium additives on hydrogen sorption of $LiH–MgB_2$ composite in order to find suitable chemical structure and optimal amount of the proposed dopant. In addition to that, the comparison with another type of additives (e.g Sc- or Ce-based [30] additives) will be important for general understanding of their behavior.

4. Conclusions

It can be noted that the combination of the volumetric, SR-PXD and spectroscopic techniques gives a comprehensive description of reactive hydride composites. In present work, we studied the effects of titanium-based additives on hydrogen absorption-desorption properties of $2LiH–MgB_2$ composite. We found that:

(i) All the systems with additives showed an improvement of reaction rate, especially for hydrogen desorption. In case of TiO_2, the composite demonstrated the best kinetics for both hydrogen absorption and desorption (~ 7.6 wt % H_2 in ~ 1.8 h and 2.7 h, respectively). Moreover, hydrogen storage capacity of $LiH–MgB_2–TiO_2$ system, during five sorption cycles, was only slightly reduced by ~ 0.6 wt % H_2 with respect to that of the unmodified $LiH–MgB_2$.

(ii) For all composites, hydrogen desorption was observed through intermediate step of reaction (1) with the formation of pure magnesium. For $LiH–MgB_2–TiO_2$ composite, magnesium phase was present during a short time and almost complete hydrogen sorption was confirmed after 2 h at 380 ºC.

(iii) IR analysis has shown the presence of peaks due to $[BH_4]^-$, proving the $LiBH_4$ formation after hydrogen absorption of the all composites. The spectrum of the ball-milled $LiH–MgB_2–TiF_4$ did not exhibit any peaks due to TiF_4, neither after ball milling nor after 1-st hydrogen absorption. The baselines of the spectra of hydrogenated $LiH–MgB_2–X$ (X = TiF_4, TiO_2, TiN and TiC) systems indicate the presence of MgH_2.

(iv) Only TiF_4 additive was chemically active in the composite and consequently new phases (LiF and TiB_2) were detected by SR-PXD measurements. For other $LiH–MgB_2–X$ systems (X = TiO_2, TiN and TiC) titanium-based additives were chemically inert during the entire experiment. It means that TiO_2, TiN and TiC did not react during hydrogen sorption and apparently they could be responsible for kinetic effect as catalysts.

Acknowledgements

Corresponding author thanks Dr. P. Moretto for a good management at the measurements at JRC, Petten and Dr. M. Tolkiehn for a technical support at DESY, Hamburg. Present work was supported by the European Commission (contract MRTN-CT-2006-035366).

REFERENCES

[1] Züttel A, Wenger P, Rentsch S, Sudan P. $LiBH_4$ a new hydrogen storage material. J Power Sources 2003; 118:1–7.

[2] Barkhordarian G, Klassen T, Dornheim M, Bormann R. Unexpected kinetic effect of MgB_2 in Reactive Hydride Composites containing complex borohydrides. J Alloys Comp 2007;440:L18–21.

[3] Bösenberg U, Doppiu S, Mosegaard L, Barkhordarian G, Eigen N, Borgschulte A, Jensen TR, Cerenius Y, Gutfleisch O, Klassen T, Dornheim M, Bormann R. Hydrogen sorption properties of MgH_2+2$LiBH_4$. Acta Mater 2007;55:3951–58.

[4] Bogdanovic B, Schwickardi M. Ti-doped alkali metal aluminium hydrides as potential novel reversible hydrogen storage materials. J Alloys Comp1997;253:1–9.

[5] Wang P, Ma L, Fang Z, Kang X, Wang P. Improved hydrogen storage property of Li–Mg–B–H system by milling with titanium trifluoride. Energy Environ Sci 2009;2:120–3.

[6] Deprez E, Munoz-Marquez MA, Roldan MA, Prestipino C, Palomares FJ, Bonatto-Minella Ch, Bösenberg U, Dornheim M, Bormann R, Fernandez A. Oxidation state and local structure of Ti-based additives in the reactive hydride composite of $2LiBH_4+MgH_2$. J Phys Chem C 2010;114:3309–17.

[7] Bösenberg U. $LiBH_4+MgH_2$ composites for hydrogen storage. PhD–Thesis, Geesthacht: GKSS-Forschungszentrum Geesthacht GmbH; 2009.

[8] Bösenberg U, Kim JW, Gosslar D, Eigen N, Jensen TR, Belosta von Colbe J, Zhou Y, Damhs M, Kim DH, Günther R, Cho YW, Oh KH, Klassen T, Bormann R, Dornheim M. Role of additives in $LiBH_4$–MgH_2 reactive hydride composites for sorption kinetics. Acta Mater 2010;58:3381–89.

[9] Łodziana Z, Züttel A, Zielinski P. Titanium and native defects in $LiBH_4$ and $NaAlH_4$. J Phys Con Matter 2008; 20:465210.

[10] Bösenberg U, Tolkeihn M, Pistidda C, Saldan I, Suarez-Alcantara K, Arendarska A, Klassen T, Dornheim M. Characterization of metal hydrides with in-situ XRD. J App Crystallography 2011; In press.

[11] Yan-Ping Zhou. Catalyst optimization for $LiBH_4+MgH_2$ composite. MSc–Thesis, Geesthacht: GKSS–Forschungszentrum Geesthacht GmbH; 2007.

[12] Parker SF. Spectroscopy and bonding in ternary metal hydride complexes – potential hydrogen storage media. Coordination Chem. Rev. 2010;254;215–234.

[13] Nakamoto K. Infrared and Raman Spectra of Inorganic and Coordination Compounds. Part A. In: Theory and Applications in Inorganic Chemistry, 6th ed. New Jersey: Wiley & Sons Inc; 2009, p. 119–129.

[14] Mosegaard L, Møller B, Jørgensen J-E, Filinchuk Ya, Cerenius Y, Hanson J, Dimasi E, Besenbacher F, Jensen TR. Reactivity of $LiBH_4$: in situ synchrotron radiation powder X-ray diffraction study. J Phys Chem C 2008;112:1299–1303.

[15] Au M, Jurgensen A. Modified Lithium Borohydrides for Reversible Hydrogen Storage. J Phys Chem B 2006;110:7062–67.

[16] Hoekstra H, Katz J. The Preparation and Properties of the Group IV-B Metal Borohydrides. J Am Chem Soc 1949;71:2488–92.

[17] Au M, Jurgensen A, Zeigler K. Modified Lithium Borohydrides for Reversible Hydrogen Storage (2). J Phys Chem B 2006;110:26482–87.

[18] Varin RA, Zbroniec L. The effects of ball milling and nanometric nickel additive on the hydrogen desorption from lithium borohydride and manganese chloride ($3LiBH_4 + MnCl_2$) mixture. J Hydrogen Energy 2010;35:3588–97.

[19] Au M, Walters RT. Reversibility aspect of lithium borohydrides. J Hydrogen Energy 2010;35:10311–16.

[20] Henrich VE, Cox PA. The surface science of metal oxides. New York: Cambridge University Press; 1994.

[21] Hummer R, Nørskov JK. Electronic factors determining the reactivity of metal surfaces. Surf Sci 1995; 343:211–20.

[22] Hummer R, Nørskov JK. Why gold is the noblest of all the metals. Nature 1995;376:238–40.

[23] Barkhordarian G, Klassen T, Bormann R. Effect of Nb_2O_5 content on hydrogen reaction kinetics of Mg. J Alloys Comp 2004;364:242–46.

[24] Barkhordarian G, Klassen T, Bormann R. Catalytic mechanism of transition-metal compounds on Mg hydrogen sorption reaction. J Phys Chem B 2006;110:11020–24.

[25] Borgschulte A, Bösenberg U, Barkhordarian G, Dornheim M, Bormann R. Enhanced hydrogen sorption kinetics of magnesium by destabilized $MgH_{2-\delta}$. Cat Today 2007; 120:262–69.

[26] Walker GS, Williams E, Bhattacharya AK. Preparation and characterization of high surface area alumina-titania solid acids. J Mater Sci 1997;32:5583–92.

[27] Lide DR. Handbook of Chemistry and Physics. 74th ed. CRC Press;1993–1994.

[28] Zhang Y, Morin F, Huot J. The effects of Ti-based additives on the kinetics and reactions in LiH/MgB_2 hydrogen storage system. J Hydrogen Energy 2011;36:5425–30.

[29] Sridechprasat P, Suttisawat Y, Rangsunvigit P, Kitiyanan B, Kulprathipanja S. Catalyzed $LiBH_4$ and MgH_2 mixture for hydrogen storage. J Hydrogen Energy 2011;36:1200–05.

[30] Liu BH, Zhang BJ, Jiang Y. Hydrogen storage performance of $LiBH_4+1/2MgH_2$ composites improved by Ce-based additives. J Hydrogen Energy 2011;35:5418–24.

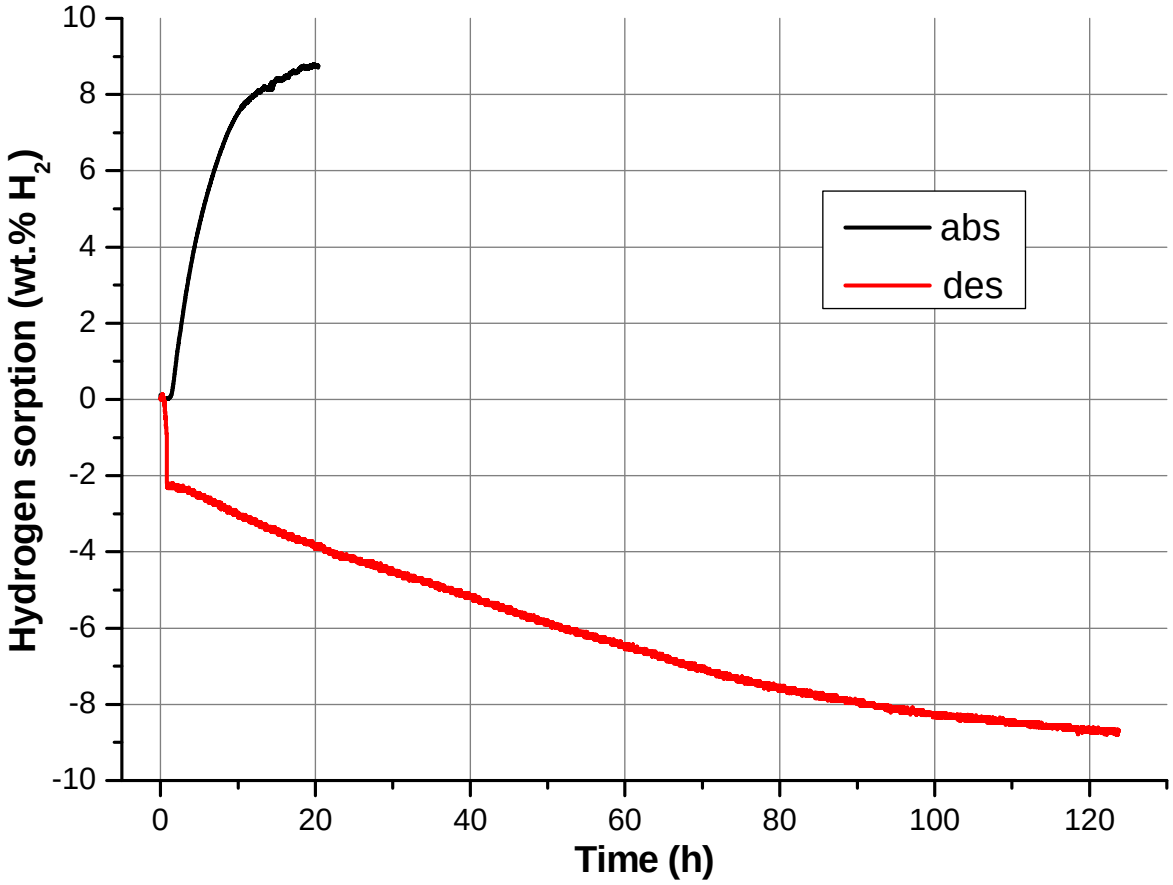

Fig.1. Hydrogen sorption for LiH–MgB_2 in molar ratio 2:1. Conditions for absorption and desorption were 350 ºC at 50 bar H_2 and 380 ºC at 5 bar H_2, respectively.

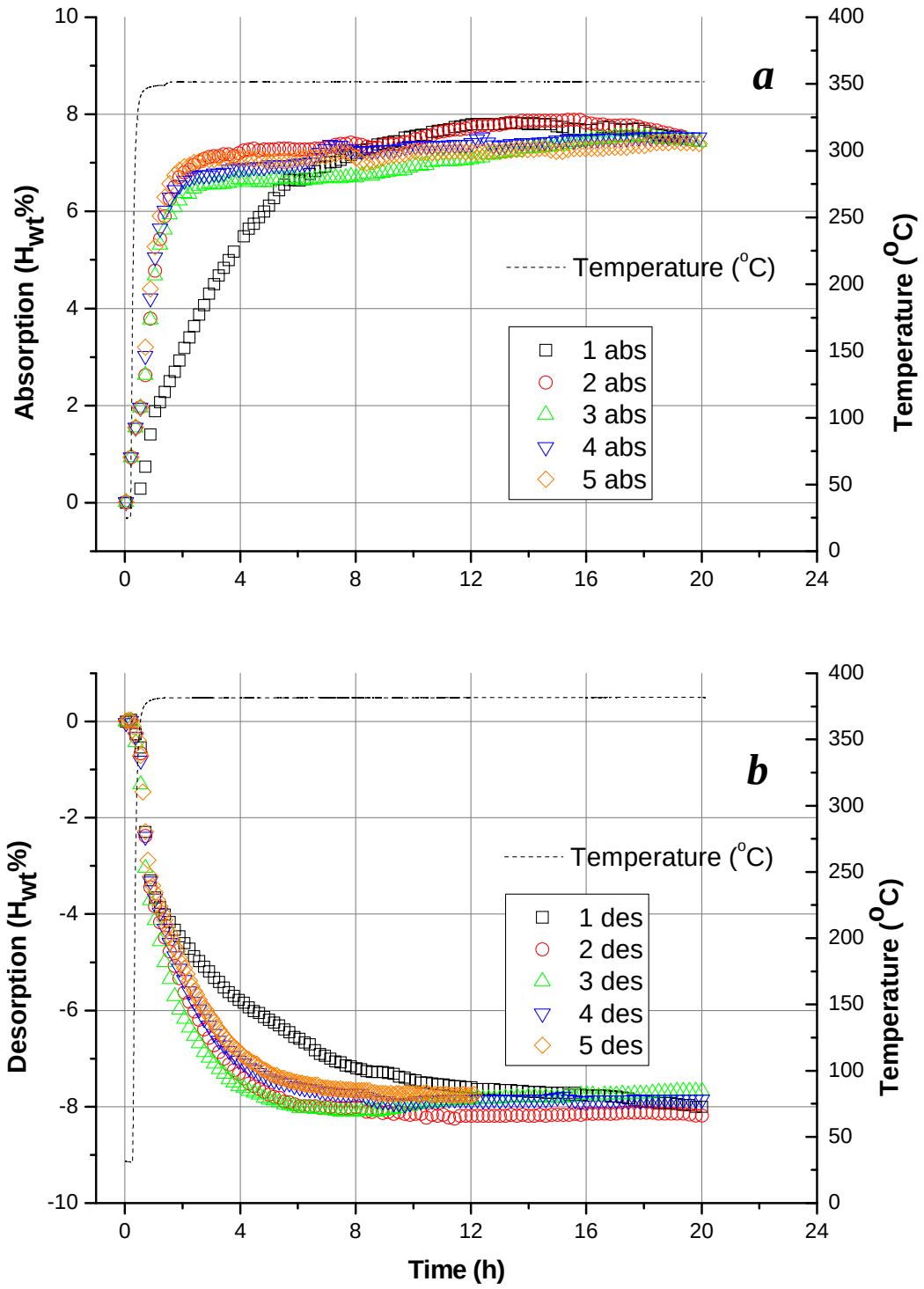

Fig.2 Hydrogen sorption for LiH–MgB_2–TiF_4 in molar ratio 2:1:0.1 during 5 cycles. Absorption (*a*) at 350 ºC and 50 bar H_2; desorption (*b*) at 380 ºC and 5 bar H_2.

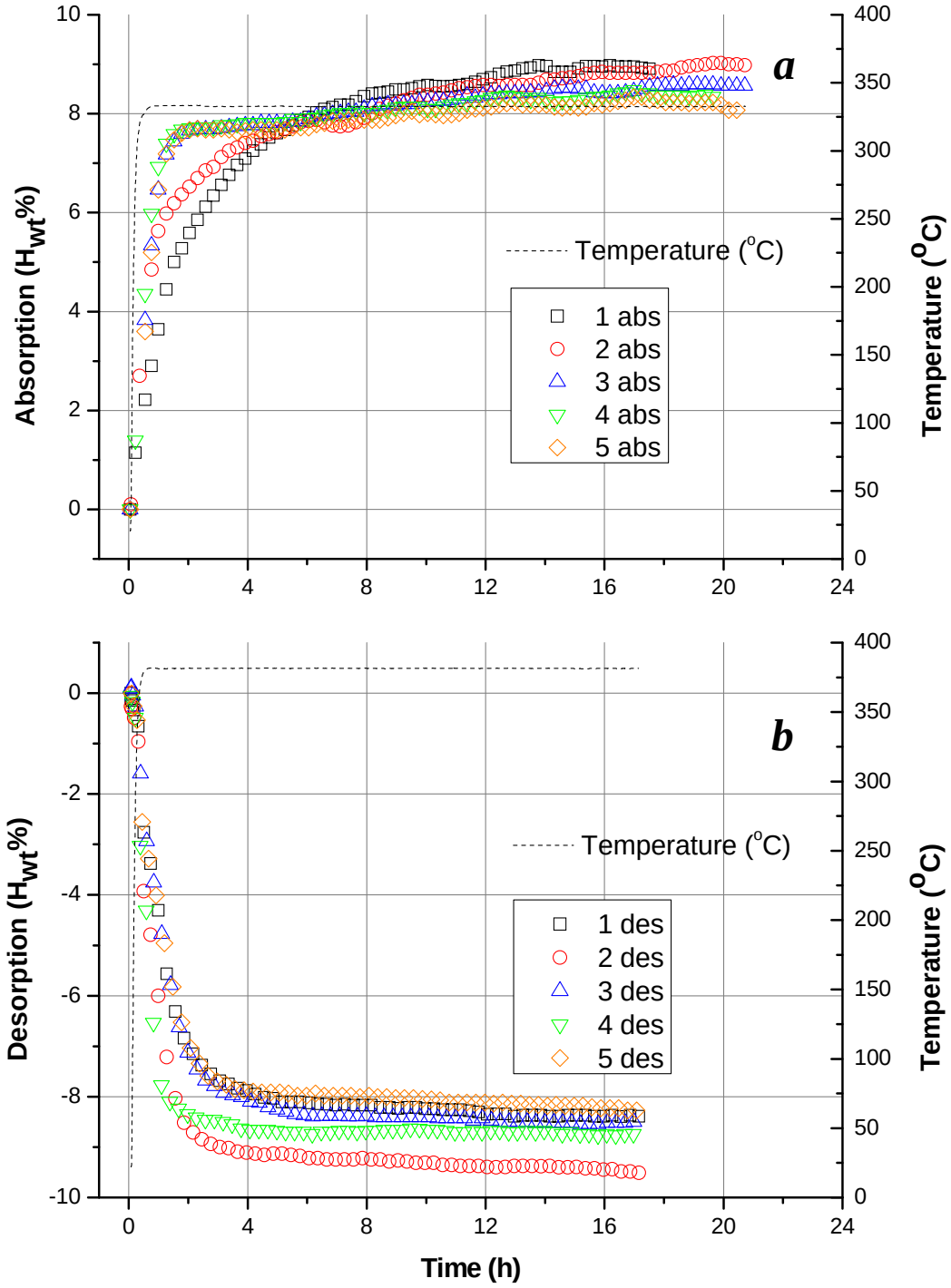

Fig.3 Hydrogen sorption for LiH–MgB_2–TiO_2(rutile) in molar ratio 2:1:0.1 during 5 cycles. Absorption (*a*) at 330 ºC and 50 bar H_2; desorption (*b*) at 380 ºC and 5 bar H_2.

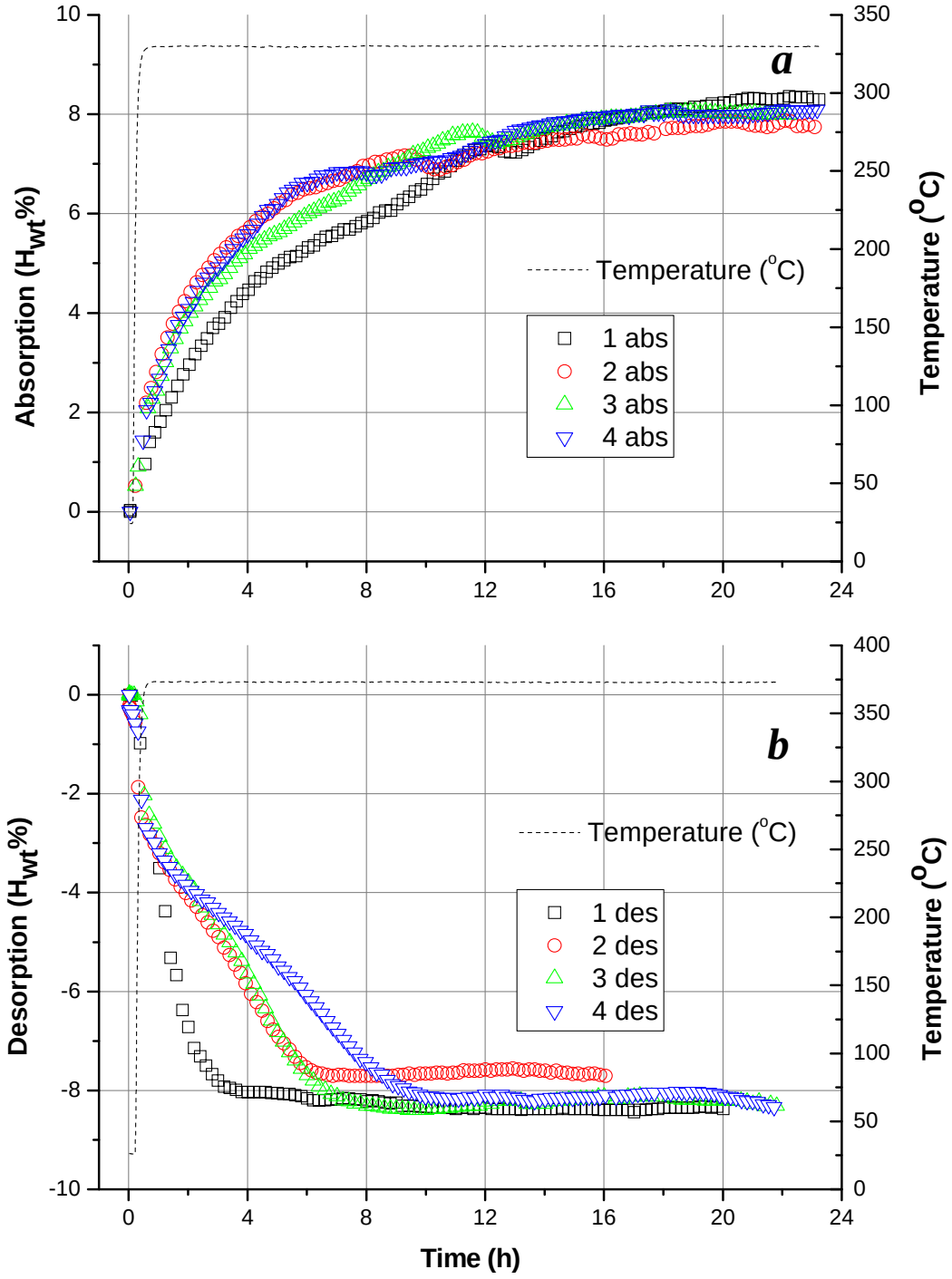

Fig.4 Hydrogen sorption for LiH–MgB_2–TiN in molar ratio 2:1:0.1 during 5 cycles. Absorption (*a*) at 330 ºC and 50 bar H_2; desorption (*b*) at 380 ºC and 5 bar H_2.

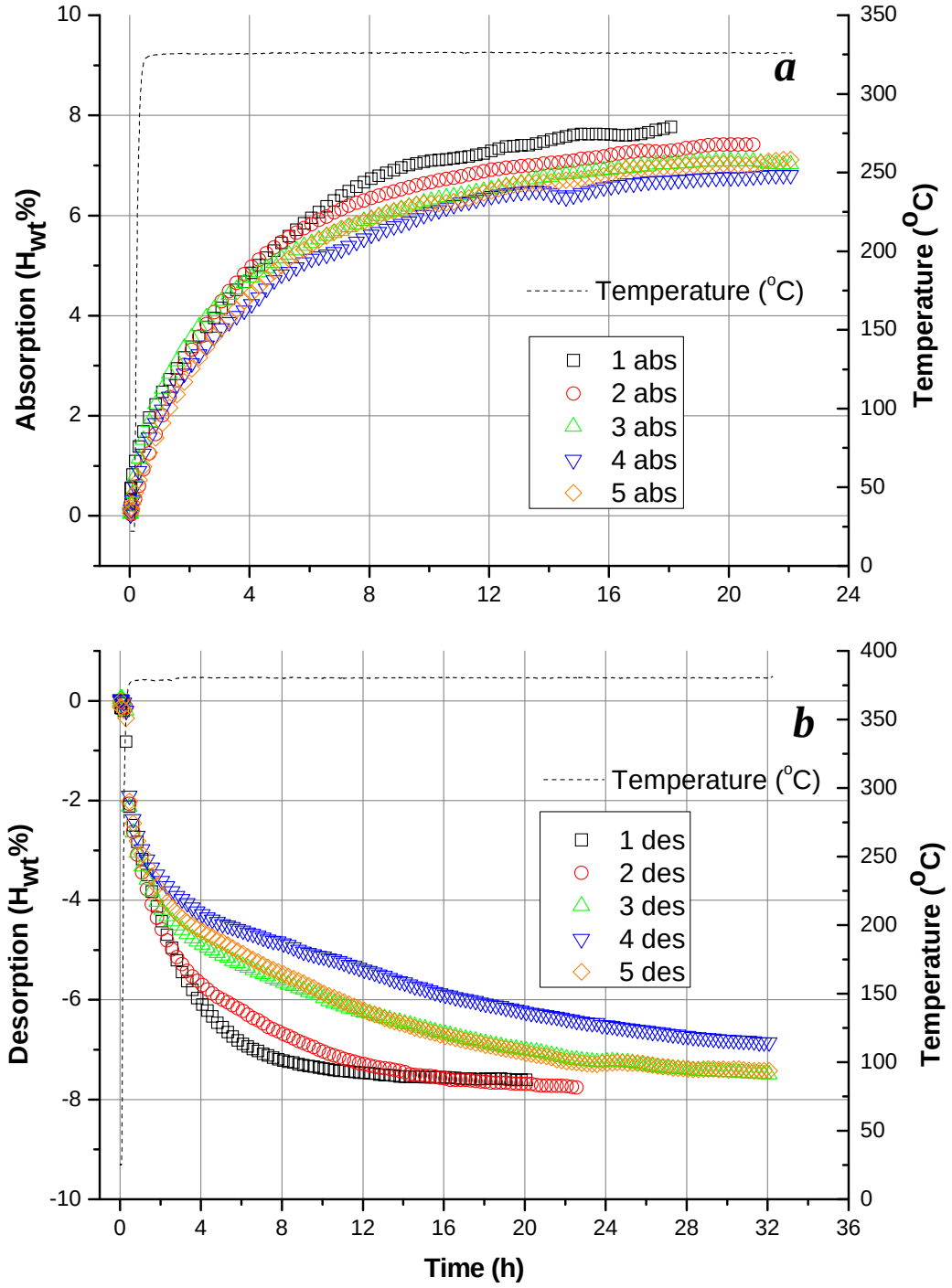

Fig.5 Hydrogen sorption for LiH–MgB_2–TiC in molar ratio 2:1:0.1 during 5 cycles. Absorption (*a*) at 330 ºC and 50 bar H_2; desorption (*b*) at 380 ºC and 5 bar H_2.

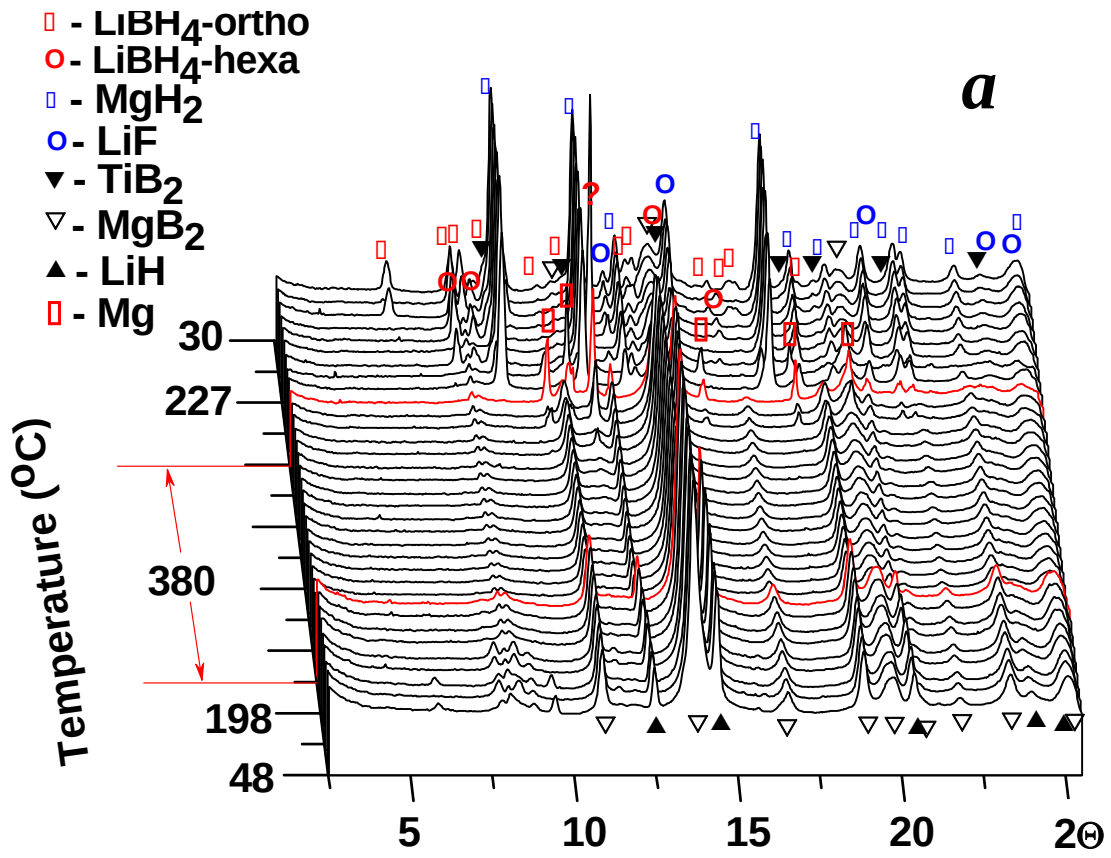
- LiBH4-ortho
- LiBH4-hexa
- MgH2
- LiF
- TiB2
- MgB2
- LiH
- Mg
a
Temperature (°C)
30
227
380
198
48
5
10
15
20
2Θ

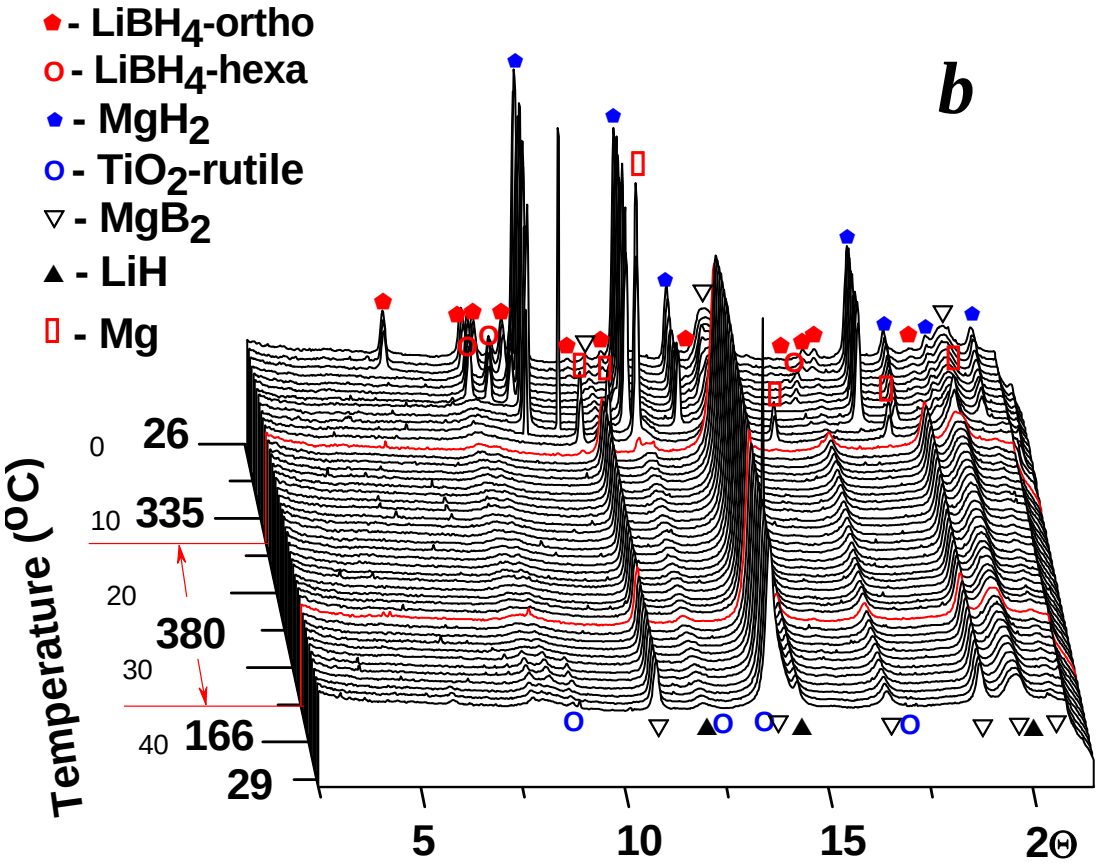
- LiBH4-ortho
- LiBH4-hexa
- MgH2
- TiO2-rutile
- MgB2
- LiH
- Mg
b
Temperature (°C)
0
26
10
335
20
380
30
166
40
29
5
10
15
2Θ

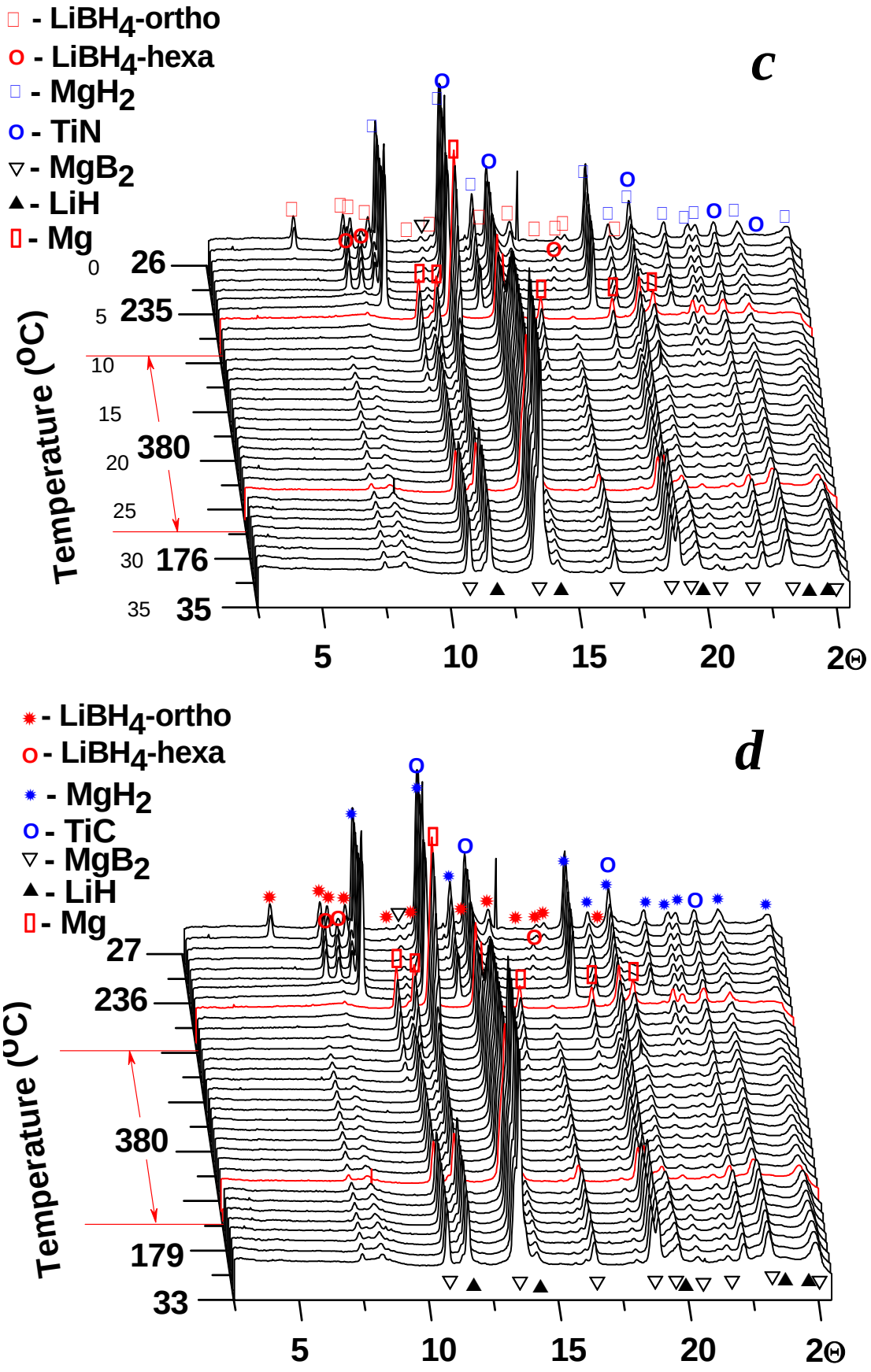

Fig. 6 In-situ SR-PXD under 5 bar H_2 for LiH–MgB_2–TiX (X = TiF_4 (*a*); TiO_2 (*b*); TiN (*c*); TiC (*d*)) in molar ratio 2:1:0.1 composites after complete 1-st hydrogen absorption.

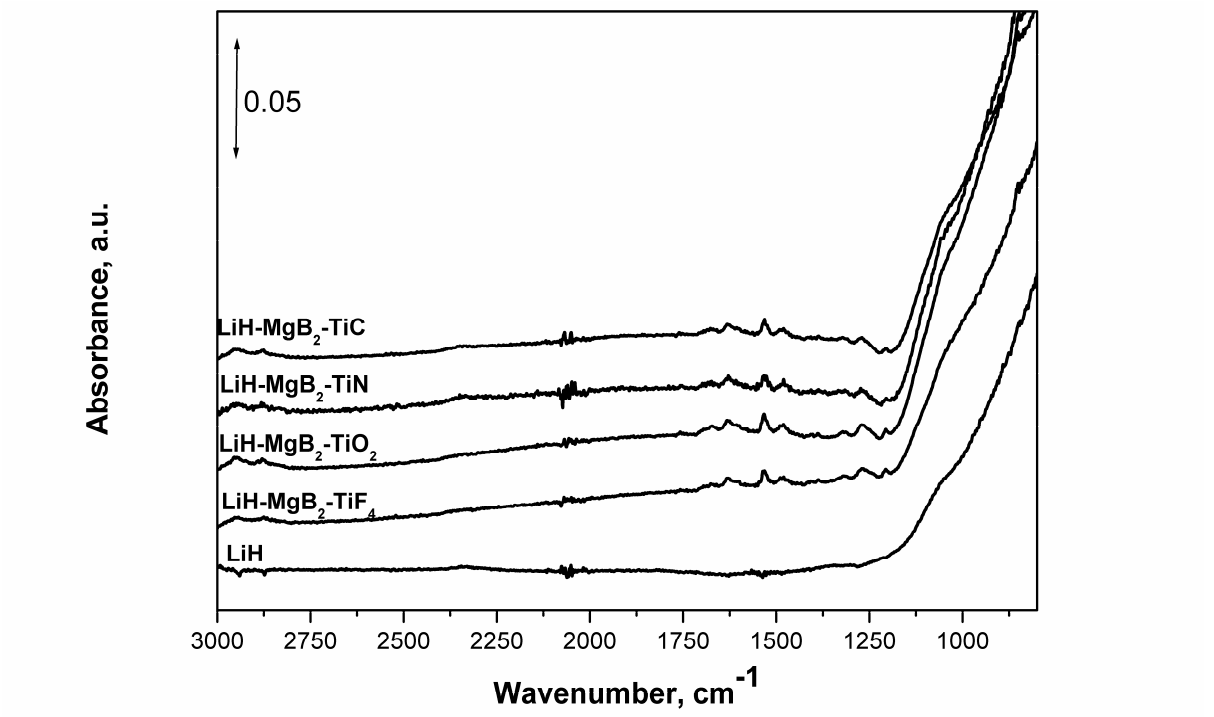

Fig.7 ATR-IR spectra of LiH–MgB_2–X (X = TiF_4, TiO_2, TiN, TiC) systems after ball-milling. The reference spectrum of LiH is also shown. Spectra are translated along the Y axis for better representation.

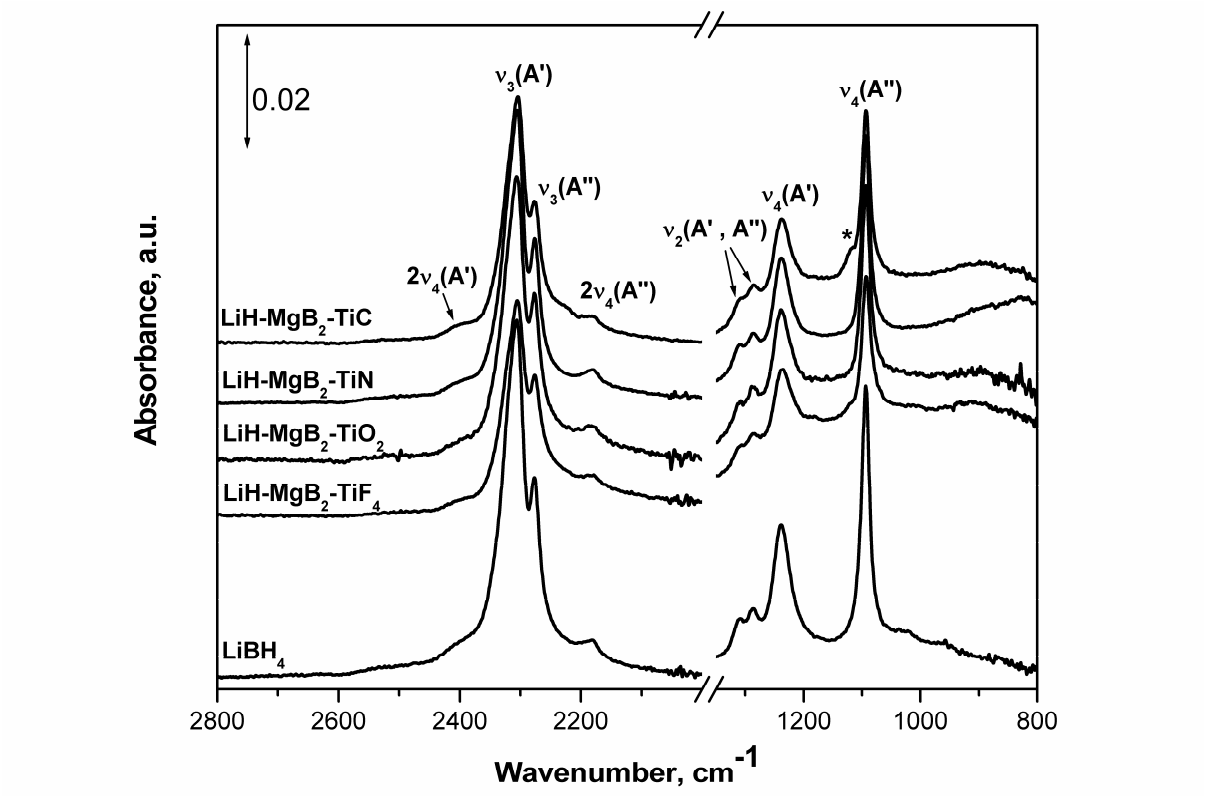

Fig.8. ATR-IR spectra of LiH–MgB_2–X (X = TiF_4, TiO_2, TiN, TiC) systems after 1st hydrogen absorption. The reference spectrum of $LiBH_4$ is also shown. Spectra are translated along the Y axis for better representation.

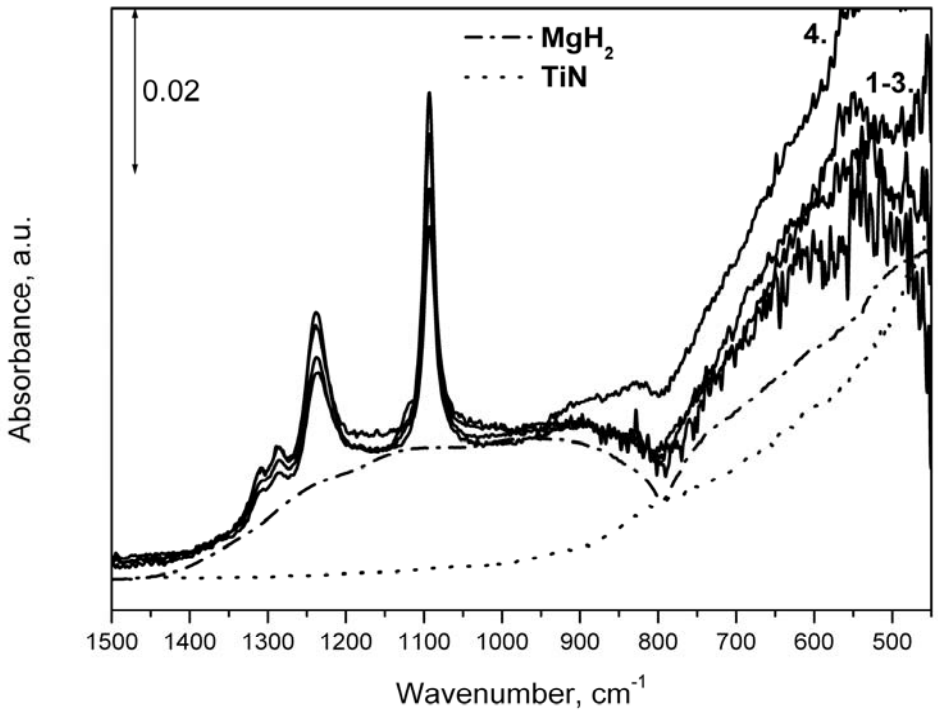

Fig.9. ATR-IR spectra in low region of LiH–MgB_2–X (X = TiF_4, TiO_2, TiN, TiC) systems after 1st hydrogen absorption: spectra 1-3 correspond to the composites with TiO_2, TiC, and TiF_4, respectively, spectrum 4 corresponds to the composite with TiN additive.

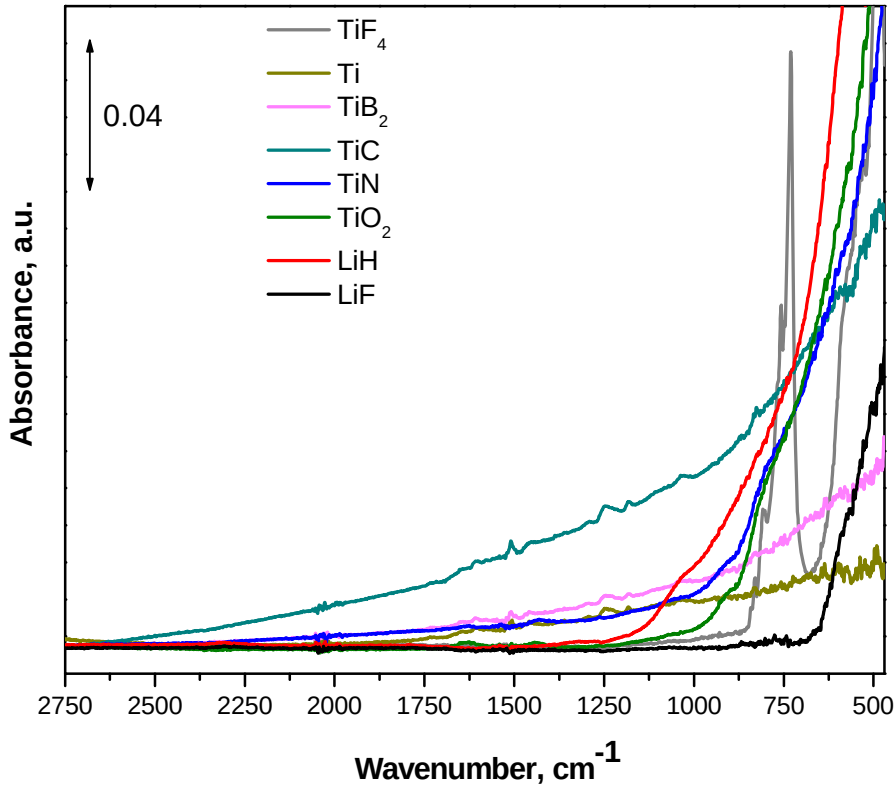

Figure S1. ATR-IR spectra of reference compounds.